

## Energy Dissipation Rate Control Via a Semi-Analytical Pattern Generation Approach for Planar Three-Legged Galloping Robot based on the Property of Passive Dynamic Walking

M. Azimi<sup>1</sup>, M. R. Hairi Yazdi<sup>2\*</sup>

1. M.Sc. Student, School of Mechanical Engineering College of Engineering, University of Tehran, Tehran, Iran

2. Associate Professor, School of Mechanical Engineering College of Engineering, University of Tehran, Tehran, Iran

Received 8 July 2014; Accepted 20 September 2014

### Abstract

In this paper an Energy Dissipation Rate Control (EDRC) method is introduced, which could provide stable walking or running gaits for legged robots. This method is realized by developing a semi-analytical pattern generation approach for a robot during each Single Support Phase (SSP). As yet, several control methods based on passive dynamic walking have been proposed by researchers to provide an efficient human-like biped walking robot. For most of these passive based controllers the main idea is to shape the robot's energy level during each SSP to restore the mechanical energy which has been lost in the previous Impact Phases (IP); however, the EDRC method provides stable gaits for legged robots just by controlling the robot's energy level during each IP. In this paper EDRC is applied to a Six-Link Three-Point Foot (6L3PF) model, to realize an active dynamic galloping gait on level ground. As the point-foot contact assumption for the 6L3PF imposes one degree of under-actuation in the ankle joint, it is not clear how to specify the forward kinematic defining the swing leg position and velocity as a function of actuated joint angles. So, a new strategy for solving the dynamic and kinematic equations of the robot is introduced for deriving suitable joint trajectories during each SSP. Simulation results show that the proposed methods in this paper are effective and the robot exhibits a stable dynamic galloping gait on level ground.

**Keywords:** *Inverted Pendulum Model (IPM), passive dynamic walking, point-foot contact assumption, semi-analytical pattern generation.*

### 1. Introduction

Passive dynamic walking, as proposed by McGeer, is known as the most energy-efficient approach, in which a biped robot walks down a gentle slope continuously and stably just by utilizing its natural dynamics [1,2]. But deployment of such robots is faced with problems. On one hand steady gait cannot be

obtained easily without suitable parameter choice; on the other, steady gait is very sensitive to initial states and ground slope [3]. To overcome these problems, the concept of passive based controllers was developed, which uses the minimal actuations such as ankle torque or hip torque to achieve stable limit cycle [4]. Consequently, several researchers have shown their interest in the applications of passive dynamic walking to

\* Corresponding Author, Tel: +980912111541  
Email: myazdi@ut.ac.ir

realize efficient dynamic walking on level ground. For most of these passive based controllers, the pattern-generation mechanism during each SSP is based on the idea of restoring the mechanical energy which has been lost in the previous IPs, for example energy shaping control [5,6], virtual gravity control [7–10], or parametric excitation control [11]. But this is a complicated task, as during each SSP the total mechanical energy of the robot is a function of the robot's position and velocity simultaneously. Also, controlling the robot's energy level during SSP makes the walking pattern almost arbitrary. Based on the fact that during an IP, the robot does not exhibit significant movements and the level of mechanical energy is just a function of the robot's velocity, in this paper the EDRC method is introduced, which proposes the idea of controlling the amount of energy lost in each IP by controlling the robot's velocity just before each IP. Also, elimination of the robot's energy-level constraint enables us to control the robot's walking pattern during each SSP, which is very desirable for robots that work on irregular terrains.

As mentioned above, applying the EDRC method demands exact control of swing-limb velocity just before each IP, but for legged robots with point-foot contact assumption there is no actuation at the ankle joint. Therefore, there is no direct control over the foot angle with the ground, and it is not clear how to specify the forward kinematics defining the swing-limb position and velocity as a function of actuated joint angles [12]. In fact, in such mechanisms the kinematic equations of the actuated element are coupled to the dynamic equations of the under-actuated elements. This paper therefore introduces how the kinematic and dynamic equations of a 6L3PF robot with one degree of under-actuation in the ankle joint could be written as an Ordinary Differential Equation (ODE) system to generate suitable trajectories for actuated joint during each SSP. Also, the uniqueness of this ODE's answer avoids any redundancy problem during the pattern generation.

The rest of this paper is organized as follows. Section II introduces mechanical structure and galloping methodology. Section III describes dynamic equations of the robot for SSP. Section IV explains the proposed semi-analytical

trajectory-generation algorithms. Section V presents control law and stability criteria, and finally in section VI effectiveness of the proposed methods is examined by numerical simulations. Results show that the proposed under-actuated quadruped robot can gallop on level ground, firmly and continuously.

## 2. Model Description

### 2.1. Mechanical Structure

Figure 1 shows the model of the planar quadruped robot dealt with in this paper. This mechanical arrangement consists of one torso and three separate legs, such that there is a thigh, a shank, and a point foot ( $m_{ST}/m_{SW}^F$ ) for each one of the fore legs, and a leg and a point foot ( $m_{SW}^H$ ) for the hind leg. Physical parameters for each rigid link (torso/leg/thighs/shanks) include the mass ( $m_i$ ), the length ( $L_i$ ), the distance between the centre of mass and distal point ( $a_i$ ), and the inertia moment ( $I_i$ ). Also, this robot is composed of six frictionless pin joints ( $\theta_i$ ,  $i=1, 2, 3, 4, 5, 6$ ) measured counter clock-wise (CCW) with respect to the horizontal line. They are introduced separately as: stance ankle joint ( $J_1$ ), connecting the foot and the shank of the stance leg together; stance knee joint ( $J_2$ ), connecting the shank and the thigh of the stance leg together; shoulder joint ( $J_3$ ), connecting the swing-fore-leg and the stance leg together; swing knee joint ( $J_4$ ), connecting the thigh and the shank of the swing-fore-leg together; torso joint ( $J_5$ ), connecting the torso and the stance leg together; and hip joint ( $J_6$ ), connecting the swing-hind-leg and the torso together.

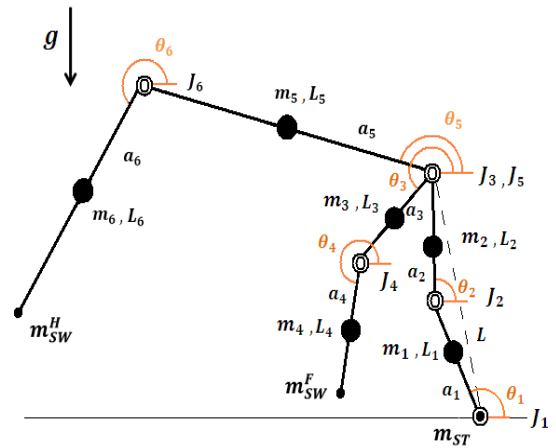


Fig. 1. Six-Link Three-Point Mass (6L3PM) Model

During each SSP the stance knee joint ( $J_2$ ) is assumed to be locked with an offset and via a knee stopper to avoid the singularity problem in analytical calculation. So, during each SSP the stance leg is considered as a conjunct link with virtual length of  $L$ , as represented by the dashed line in Figure 1.

$$\theta_2 - \theta_1 = \varphi, \quad \varphi > 0 \quad (1)$$

## 2.2. Bouncing methodology

In this article no Double Support Phase (DSP) is considered; therefore a complete cycle of galloping gait is composed of one Jump-Off (JO), one Flight Phase (FP), one Touch-Down (TD), two SSP, and two IP. A complete cycle of galloping starts with a JO such that the angular velocity of the joints increase during a very short time, after which the robot enters FP such that the whole robot behaves as a ballistic throw; FP ends by a plastic collision between the fore feet and the ground as TD. After that, during the first SSP, one of the fore legs is considered as an IPM, stance leg, which rotates around its contact point passively [13,14]; on the one hand the whole torso and hind leg and on the other hand the swing-fore-leg are considered as two Fully-Actuated-Double-Pendulum-Model (FADPM) mounted at hip level of the stance leg. In this manner, during the SSP the hind leg, torso and swing-fore-leg come forward fully actuated, while the stance leg rotates around its contact point passively. As soon as the swing-fore-foot reaches the ground, the first SSP ends and the first IP takes place instantaneously. During IP a completely plastic collision occurs between the swing-fore-foot and the ground, and the velocity of the elements change [15]. The second SSP starts just after the first IP. As in the first SSP, the hind leg and the torso act as a FADPM, but the role of swing and stance leg is exchanged between the two fore legs. This whole cycle repeats continuously to produce a galloping gait.

## 3. Driving the Dynamic Equation

Since during both SSPs the stance knee joint is locked, the whole robot is to be considered as an open kinematic chain with five links and five Degrees of Freedom (DOF). Therefore, using the well-known Newton's Second Law

or the Euler-Lagrange approach, dynamic equations of the model can be obtained as:

$$M(\theta)\ddot{\theta} + C(\theta, \dot{\theta})\dot{\theta} + g(\theta) = ST \quad (2)$$

where  $\theta = [\theta_1, \theta_3, \theta_4, \theta_5, \theta_6]^T$  is the generalized coordinate vector of the robot,  $M(\theta) = [5 \times 5]$  is the inertia matrix,  $C(\theta, \dot{\theta}) = [5 \times 5]$  is the centripetal and coriolis forces matrix, and  $g(\theta) = [5 \times 1]$  is the gravitational effects vector. Also,  $T = [0T_3T_4T_5T_6]^T$  represents the generalized internal torque vector, and  $S = [5 \times 5]$  is a matrix which selects the actuator torques for each segment such that  $T_3, T_4, T_5$  and  $T_6$  appear at the shoulder joint ( $J_3$ ), the swing knee joint ( $J_4$ ), the torso joint ( $J_5$ ), and the hip joint ( $J_6$ ) respectively.

$$S = \begin{bmatrix} 1 & -1 & 0 & -1 & 0 \\ 0 & 1 & -1 & 0 & 0 \\ 0 & 0 & 1 & 0 & 0 \\ 0 & 0 & 0 & 1 & -1 \\ 0 & 0 & 0 & 0 & 1 \end{bmatrix} \quad (3)$$

## 4. Trajectory Generation

Using the kinematic and dynamic equations of the robot during SSP, here a systematic approach is presented to generate robot trajectories from the solution of an ODE system.

### 4.1. Dynamic analysis

Equation (2) contains five coupled ODEs. By eliminating  $T_3, T_4, T_5$  and  $T_6$  in these five equations:

$$f(\theta_1, \theta_3, \theta_4, \theta_5, \theta_6, \dot{\theta}_1, \dot{\theta}_3, \dot{\theta}_4, \dot{\theta}_5, \dot{\theta}_6, \ddot{\theta}_1, \ddot{\theta}_3, \ddot{\theta}_4, \ddot{\theta}_5, \ddot{\theta}_6) = 0 \quad (4)$$

This is an ODE with five unknowns ( $\theta_i, i=1,3,4,5,6$ ) where four more equations needs to be solved. In the following describes how the kinematic equations of the robot are used to form these four extra equations.

### 4.2. Kinematic analysis

If  $[x_{SW}^F, y_{SW}^F]^T$  and  $[x_{SW}^H, y_{SW}^H]^T$  represent the position of the swing-fore-foot and swing-

hind-foot, respectively, and the origin of the local coordinate system lies in the stance foot's ankle, as depicted in Figure 1. The position of the swing feet could be written as:

$$\begin{aligned} x_{SW}^F &= q_1(\theta_1, \theta_3, \theta_4) \\ y_{SW}^F &= q_2(\theta_1, \theta_3, \theta_4) \end{aligned} \quad (5)$$

$$\begin{aligned} x_{SW}^H &= q_3(\theta_1, \theta_5, \theta_6) \\ y_{SW}^H &= q_4(\theta_1, \theta_5, \theta_6) \end{aligned} \quad (6)$$

By differentiating Equations (5) and (6) the velocity and acceleration of swing feet can be written as:

$$\begin{aligned} \dot{x}_{SW}^F &= q_5(\theta_1, \theta_3, \theta_4, \dot{\theta}_1, \dot{\theta}_3, \dot{\theta}_4) \\ \dot{y}_{SW}^F &= q_6(\theta_1, \theta_3, \theta_4, \dot{\theta}_1, \dot{\theta}_3, \dot{\theta}_4) \end{aligned} \quad (7)$$

$$\begin{aligned} \ddot{x}_{SW}^F &= q_7(\theta_1, \theta_3, \theta_4, \dot{\theta}_1, \dot{\theta}_3, \dot{\theta}_4, \ddot{\theta}_1, \ddot{\theta}_3, \ddot{\theta}_4) \\ \ddot{y}_{SW}^F &= q_8(\theta_1, \theta_3, \theta_4, \dot{\theta}_1, \dot{\theta}_3, \dot{\theta}_4, \ddot{\theta}_1, \ddot{\theta}_3, \ddot{\theta}_4) \end{aligned} \quad (8)$$

$$\begin{aligned} \dot{x}_{SW}^H &= q_9(\theta_1, \theta_5, \theta_6, \dot{\theta}_1, \dot{\theta}_5, \dot{\theta}_6) \\ \dot{y}_{SW}^H &= q_{10}(\theta_1, \theta_5, \theta_6, \dot{\theta}_1, \dot{\theta}_5, \dot{\theta}_6) \end{aligned} \quad (9)$$

$$\begin{aligned} \ddot{x}_{SW}^H &= q_{11}(\theta_1, \theta_5, \theta_6, \dot{\theta}_1, \dot{\theta}_5, \dot{\theta}_6, \ddot{\theta}_1, \ddot{\theta}_5, \ddot{\theta}_6) \\ \ddot{y}_{SW}^H &= q_{12}(\theta_1, \theta_5, \theta_6, \dot{\theta}_1, \dot{\theta}_5, \dot{\theta}_6, \ddot{\theta}_1, \ddot{\theta}_5, \ddot{\theta}_6) \end{aligned} \quad (10)$$

By taking  $\begin{bmatrix} \ddot{x}_{SW}^F \\ \ddot{y}_{SW}^F \end{bmatrix}$  and  $\begin{bmatrix} \ddot{x}_{SW}^H \\ \ddot{y}_{SW}^H \end{bmatrix}^T$  as known parameters, Equations (4), (8) and (10) make a five-ODE and five-unknown system, which can be written according to the explicit form of  $\ddot{\theta}_1$ ,  $\ddot{\theta}_3$ ,  $\ddot{\theta}_4$ ,  $\ddot{\theta}_5$  and  $\ddot{\theta}_6$  as:

$$\begin{aligned} \ddot{\theta}_1 &= f_1(\theta_1, \theta_2, \theta_3, \theta_4, \theta_5, \dot{\theta}_1, \dot{\theta}_2, \dot{\theta}_3, \dot{\theta}_4, \dot{\theta}_5, \\ &\quad \ddot{x}_{SW}^F, \ddot{y}_{SW}^F, \ddot{x}_{SW}^H, \ddot{y}_{SW}^H) \\ \ddot{\theta}_3 &= f_3(\theta_1, \theta_2, \theta_3, \theta_4, \theta_5, \dot{\theta}_1, \dot{\theta}_2, \dot{\theta}_3, \dot{\theta}_4, \dot{\theta}_5, \\ &\quad \ddot{x}_{SW}^F, \ddot{y}_{SW}^F, \ddot{x}_{SW}^H, \ddot{y}_{SW}^H) \\ \ddot{\theta}_4 &= f_4(\theta_1, \theta_2, \theta_3, \theta_4, \theta_5, \dot{\theta}_1, \dot{\theta}_2, \dot{\theta}_3, \dot{\theta}_4, \dot{\theta}_5, \\ &\quad \ddot{x}_{SW}^F, \ddot{y}_{SW}^F, \ddot{x}_{SW}^H, \ddot{y}_{SW}^H) \\ \ddot{\theta}_5 &= f_5(\theta_1, \theta_2, \theta_3, \theta_4, \theta_5, \dot{\theta}_1, \dot{\theta}_2, \dot{\theta}_3, \dot{\theta}_4, \dot{\theta}_5, \\ &\quad \ddot{x}_{SW}^F, \ddot{y}_{SW}^F, \ddot{x}_{SW}^H, \ddot{y}_{SW}^H) \\ \ddot{\theta}_6 &= f_6(\theta_1, \theta_2, \theta_3, \theta_4, \theta_5, \dot{\theta}_1, \dot{\theta}_2, \dot{\theta}_3, \dot{\theta}_4, \dot{\theta}_5, \\ &\quad \ddot{x}_{SW}^F, \ddot{y}_{SW}^F, \ddot{x}_{SW}^H, \ddot{y}_{SW}^H) \end{aligned} \quad (11)$$

### 4.3. Inverted kinematics analysis

By solving Equation (5) according to  $\theta_3$  and  $\theta_4$ , Equation (6) according to  $\theta_5$  and  $\theta_6$ , Equation (7) according to  $\dot{\theta}_3$  and  $\dot{\theta}_4$ , Equation (9) according to  $\dot{\theta}_5$  and  $\dot{\theta}_6$ , respectively:

$$\theta_3 = z_1(\theta_1, x_{SW}^F, y_{SW}^F) \quad (12)$$

$$\theta_4 = z_2(\theta_1, x_{SW}^F, y_{SW}^F)$$

$$\theta_5 = z_5(\theta_1, x_{SW}^H, y_{SW}^H) \quad (13)$$

$$\theta_6 = z_6(\theta_1, x_{SW}^H, y_{SW}^H)$$

$$\dot{\theta}_3 = z_3(\theta_1, \theta_3, \theta_4, \dot{\theta}_1, \dot{x}_{SW}^F, \dot{y}_{SW}^F) \quad (14)$$

$$\dot{\theta}_4 = z_4(\theta_1, \theta_3, \theta_4, \dot{\theta}_1, \dot{x}_{SW}^F, \dot{y}_{SW}^F)$$

$$\dot{\theta}_5 = z_7(\theta_1, \theta_5, \theta_6, \dot{\theta}_1, \dot{x}_{SW}^H, \dot{y}_{SW}^H) \quad (15)$$

$$\dot{\theta}_6 = z_8(\theta_1, \theta_5, \theta_6, \dot{\theta}_1, \dot{x}_{SW}^H, \dot{y}_{SW}^H)$$

Substituting Equation (12) into Equation (11) and Equation (14), and also substituting Equation (13) into Equations (11) and (15) have the following result:

$$\begin{aligned} \ddot{\theta}_1 &= g_1(\theta_1, \dot{\theta}_1, \dot{\theta}_3, \dot{\theta}_4, \dot{\theta}_5, \dot{\theta}_6, x_{SW}^F, y_{SW}^F, \\ &\quad x_{SW}^H, y_{SW}^H, \ddot{x}_{SW}^F, \ddot{y}_{SW}^F, \ddot{x}_{SW}^H, \ddot{y}_{SW}^H) \\ \ddot{\theta}_3 &= g_2(\theta_1, \dot{\theta}_1, x_{SW}^F, y_{SW}^F, \dot{x}_{SW}^F, \dot{y}_{SW}^F) \\ \ddot{\theta}_3 &= g_1(\theta_1, \dot{\theta}_1, \dot{\theta}_3, \dot{\theta}_4, \dot{\theta}_5, \dot{\theta}_6, x_{SW}^F, y_{SW}^F, \\ &\quad x_{SW}^H, y_{SW}^H, \ddot{x}_{SW}^F, \ddot{y}_{SW}^F, \ddot{x}_{SW}^H, \ddot{y}_{SW}^H) \\ \ddot{\theta}_4 &= g_2(\theta_1, \dot{\theta}_1, x_{SW}^F, y_{SW}^F, \dot{x}_{SW}^F, \dot{y}_{SW}^F) \\ \ddot{\theta}_4 &= g_1(\theta_1, \dot{\theta}_1, \dot{\theta}_3, \dot{\theta}_4, \dot{\theta}_5, \dot{\theta}_6, x_{SW}^F, y_{SW}^F, \\ &\quad x_{SW}^H, y_{SW}^H, \ddot{x}_{SW}^F, \ddot{y}_{SW}^F, \ddot{x}_{SW}^H, \ddot{y}_{SW}^H) \\ \ddot{\theta}_5 &= g_2(\theta_1, \dot{\theta}_1, x_{SW}^H, y_{SW}^H, \dot{x}_{SW}^H, \dot{y}_{SW}^H) \\ \ddot{\theta}_5 &= g_1(\theta_1, \dot{\theta}_1, \dot{\theta}_3, \dot{\theta}_4, \dot{\theta}_5, \dot{\theta}_6, x_{SW}^F, y_{SW}^F, \\ &\quad x_{SW}^H, y_{SW}^H, \ddot{x}_{SW}^F, \ddot{y}_{SW}^F, \ddot{x}_{SW}^H, \ddot{y}_{SW}^H) \\ \ddot{\theta}_6 &= g_2(\theta_1, \dot{\theta}_1, x_{SW}^H, y_{SW}^H, \dot{x}_{SW}^H, \dot{y}_{SW}^H) \\ \ddot{\theta}_6 &= g_1(\theta_1, \dot{\theta}_1, \dot{\theta}_3, \dot{\theta}_4, \dot{\theta}_5, \dot{\theta}_6, x_{SW}^F, y_{SW}^F, \\ &\quad x_{SW}^H, y_{SW}^H, \ddot{x}_{SW}^F, \ddot{y}_{SW}^F, \ddot{x}_{SW}^H, \ddot{y}_{SW}^H) \end{aligned} \quad (16)$$

Considering that the stance leg functions passively:

$$\dot{\theta}_1 = \int \ddot{\theta}_1 \frac{d\theta_1}{dt} \quad (17)$$

Equation (16) could be written as a set of nonlinear state spaces, which are solvable with known initial conditions  $[\theta_1 \theta_3 \theta_4 \theta_5 \theta_6 \dot{\theta}_1 \dot{\theta}_3 \dot{\theta}_4 \dot{\theta}_5 \dot{\theta}_6]$  and a specific smooth trajectory for swing feet.

#### 4.4. Swing-feet trajectory

In this paper the swing-feet trajectories are determined by two SP-line functions. This is based on a few parameters in each SSP, such as the initial swing-foot positions and velocities, and the final desired swing-foot positions and velocities.

### 5. Control and Stability

#### 5.1. Control

A feed-forward controller is used here for controlling the robot during each SSP, which is a model-based controller with feedback from both position and velocity [16].

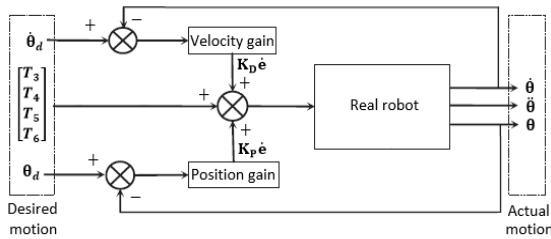


Fig. 2. Feed-forward control scheme

#### 5.2. Stability

The main difficulty in controlling legged robots is the problem of instability and the risk of falling. The first criterion for providing a stable and continuous galloping gait is mechanical energy restoration or existence of the limit cycle. In this paper an EDRC method ensured this by controlling the swing-foot velocity just before each IP. The second criterion for avoiding the robot's falling during galloping is to retain the contact-point reaction forces within an appropriate range, such that the robot's stance foot does not slip or leave the ground. Therefore, in this paper during each JO, TD, SSP and IP, the stance foot is assumed to be stuck to the ground.

### 6. Numerical Simulations

In this section the simulation results of the proposed methods are presented, using Simulink and SimMechanic toolboxes in the MATLAB program. The physical parameter values used in our numerical simulation are listed in Table 1, based on anatomical measurements of a real cheetah [17].

#### 6.1. Modelling contact point

Establishing a good contact assumption between the stance foot and the ground is the main problem in simulating the walking or running of a legged robot in digital computer software.

Table 1. Parameters of the proposed robot

Symbol	Quantity	Value
$m_1, m_4$	the forelimb's shank mass (kg)	5
$m_2, m_3$	the forelimb's thigh mass (kg)	6
$m_5$	the torso mass (kg)	48
$m_6$	the hindlimb mass (kg)	11
$m_{FF}, m_{HF}$	the point foot mass (kg)	0.5
$L_1, L_4$	the forelimb's shank length (m)	0.37
$L_2, L_3$	the forelimb's thigh length (m)	0.3
$L_2$	the torso length (m)	0.92
$L_3$	the hindlimb length (m)	0.82
$a_i$	the distance between COM and distal point (m)	$0.5 L_i$
$\phi$	the knee locking angle (deg)	10

For the point-foot contact assumption, three DOF for each robot's foot is assumed here, with two different joint blocks for the stance foot during the galloping gait, as depicted in Figure 3. Two Joint-Stiction-Actuator blocks, depicted in Figure 4, are connected to the in-plane joint. This allows locking of the joint in both x and y directions when the foot is supposed to be on the ground, and while the revolute joint is unlocked and the robot's stance leg is free to rotate around the contact point.

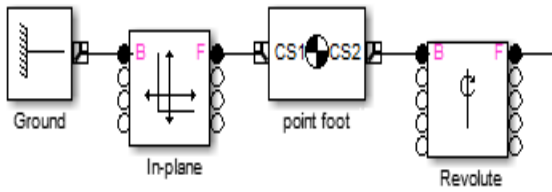


Fig. 3. Scheme of foot contact modelling

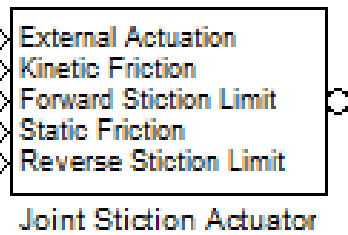


Fig. 4. A joint-stiction-actuator block

### 6.2. Numerical results

To provide a stable and steady galloping gait on level ground, it is necessary for the hind leg to have the same initial angular velocity in the beginning of each single cycle of galloping. This has been realized by choosing appropriate swing-foot velocities just before each IP. In the following the simulation results for two cycles of galloping gait are presented: the stick diagram of 6L3PM during the first and second SSPs is pictured in Figures 5a and 5b, respectively. The figures show the IPM-like behaviour of the stance leg during each SSP, where the robot's shoulder level moves on a circular curve with radius equal to the virtual length of the stance leg. Figure 6 shows the phase plane of the hind leg during these two cycles of galloping, and the graphical result of a complete cycle of galloping gait is depicted in Figure 7.

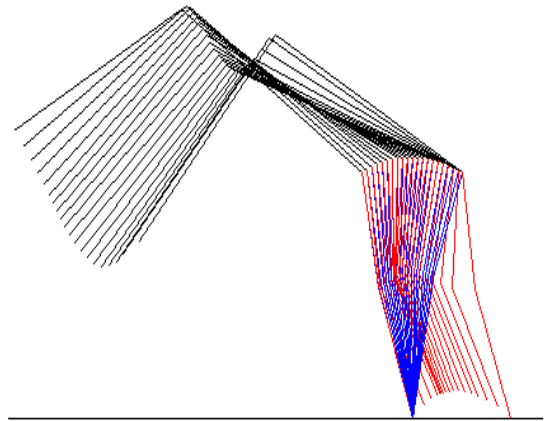


Fig. 5a. Stick diagram of 6L3PM during the first SSP

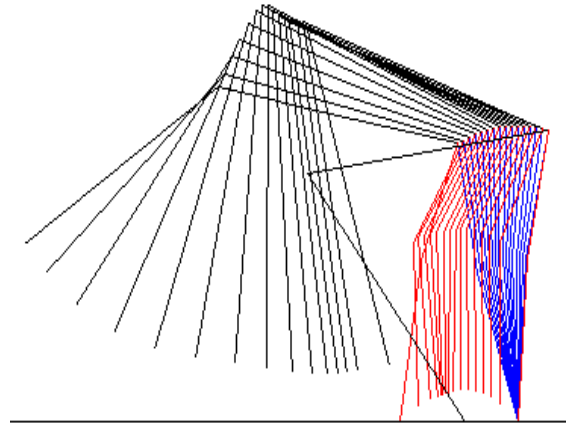


Fig. 5b. Stick diagram of 6L3PM during the second SSP

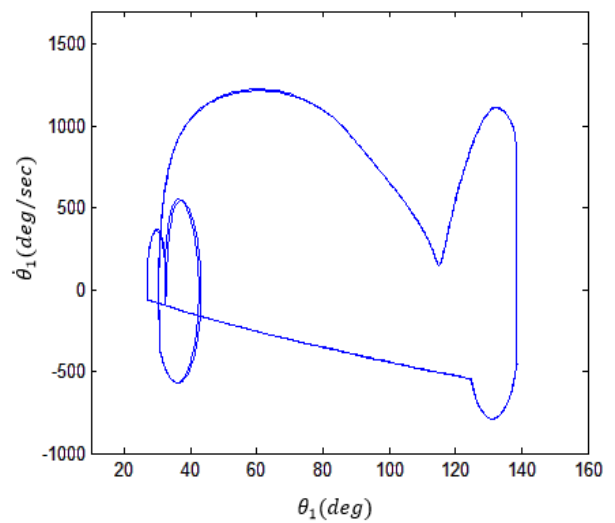


Fig. 6. The phase plane of hind limb

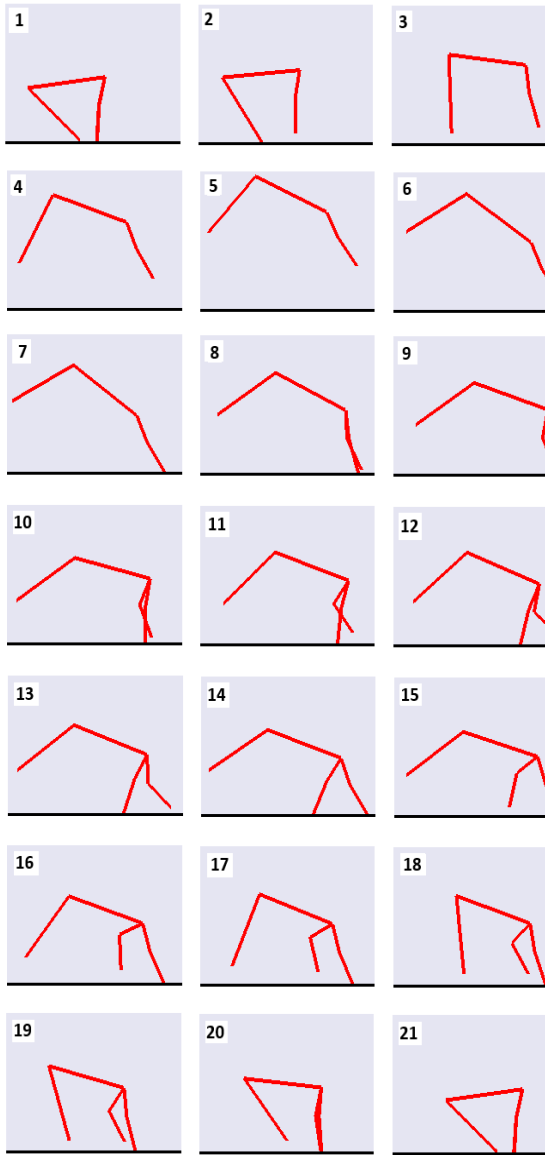


Fig. 7. Simulation of 6L3PM model

### 7. Conclusions and Future works

In this paper a 6L3PM model of a planar three-legged robot is used to gallop on level ground with 5.7848 (m/s) mean forward velocity. A new strategy is proposed to ensure the existence of limit cycle by controlling the energy dissipation rate during each IP instead of controlling the energy restoration during SSP. Also, a new semi-analytical trajectory-generation algorithm is provided for a five-linked model of the legged robot with one degree of under-actuation in the ankle joint by using the dynamic equations of the robot along with solving the inverse kinematic problem. Simulation results show that these

improvements are effective and the robot exhibits a stable dynamic galloping gait with minimum computational effort.

Since the main idea of EDRC is to control the robot's velocity during each IP, future studies should aim to derive the impact dynamic equations of the robot and solve these for different pre-impact velocities causing the desired after-impact velocities. Deriving and analysing the robot's dynamic model for phases which are not studied in this paper, like JO, FP, TD, and DSP, would also represent useful future work. The solution to Equation (16), which shows the designed robot's joint trajectories during an SSP, is just a function of designed swing-feet trajectories, which have a significant effect on the stance leg behaviour. But using SP-line function for designing swing-feet trajectories is not very desirable. Therefore, using other mathematical tools for providing suitable swing-feet trajectories is necessary in future works.

### 8. Appendix

Here the kinematic and dynamic equations of the proposed robot during an SSP are presented.

#### 8.1. Deriving kinematic equations

As depicted in Figure 1, by considering the local coordinate system mounted in the ankle joint of the stance leg, the positions of the swing feet are expressed as:

$$x_{SW}^F = L_{eq} \cos\theta_{eq} + L_3 \cos\theta_3 + L_4 \cos\theta_4 \quad (18)$$

$$y_{SW}^F = L_{eq} \sin\theta_{eq} + L_3 \sin\theta_3 + L_4 \sin\theta_4 \quad (19)$$

$$x_{SW}^H = L_{eq} \cos\theta_{eq} + L_5 \cos\theta_5 + L_6 \cos\theta_6 \quad (20)$$

$$y_{SW}^H = L_{eq} \sin\theta_{eq} + L_5 \sin\theta_5 + L_6 \sin\theta_6 \quad (21)$$

The velocities of the swing feet are obtained by differentiating Equations (18) to (21):

$$\dot{x}_{SW}^F = -L_{eq} \dot{\theta}_{eq} \sin\theta_{eq} - L_3 \dot{\theta}_3 \sin\theta_3 - L_4 \dot{\theta}_4 \sin\theta_4 \quad (22)$$

$$\dot{y}_{SW}^F = +L_{eq} \dot{\theta}_{eq} \cos\theta_{eq} + L_3 \dot{\theta}_3 \cos\theta_3 + L_4 \dot{\theta}_4 \cos\theta_4 \quad (23)$$

$$\dot{x}_{SW}^H = -L_{eq} \dot{\theta}_{eq} \sin\theta_{eq} - L_5 \dot{\theta}_5 \sin\theta_5 - L_6 \dot{\theta}_6 \sin\theta_6 \quad (24)$$

$$\dot{y}_{SW}^H = +L_{eq} \dot{\theta}_{eq} \cos\theta_{eq} + L_5 \dot{\theta}_5 \cos\theta_5 + L_6 \dot{\theta}_6 \cos\theta_6 \quad (25)$$

Similarly, the accelerations of the swing feet are obtained by differentiating Equations (22) to (25):

$$\dot{x}_{SW}^F = -L_{eq}\dot{\theta}_{eq}^2 \cos\theta_{eq} - L_3\dot{\theta}_3^2 \cos\theta_3 - L_4\dot{\theta}_4^2 \cos\theta_4 - L_{eq}\ddot{\theta}_{eq} \sin\theta_{eq} - L_3\ddot{\theta}_3 \sin\theta_3 - L_4\ddot{\theta}_4 \sin\theta_4 \quad (26)$$

$$\ddot{y}_{SW}^F = +L_{eq}\dot{\theta}_{eq}^2 \sin\theta_{eq} + L_3\dot{\theta}_3^2 \sin\theta_3 + L_4\dot{\theta}_4^2 \sin\theta_4 + L_{eq}\ddot{\theta}_{eq} \cos\theta_{eq} + L_3\ddot{\theta}_3 \cos\theta_3 + L_4\ddot{\theta}_4 \cos\theta_4 \quad (27)$$

$$\ddot{x}_{SW}^H = -L_{eq}\dot{\theta}_{eq}^2 \cos\theta_{eq} - L_3\dot{\theta}_3^2 \cos\theta_3 - L_6\dot{\theta}_6^2 \cos\theta_6 - L_{eq}\ddot{\theta}_{eq} \sin\theta_{eq} - L_3\ddot{\theta}_3 \sin\theta_3 - L_6\ddot{\theta}_6 \sin\theta_6 \quad (28)$$

$$\ddot{y}_{SW}^H = +L_{eq}\dot{\theta}_{eq}^2 \sin\theta_{eq} + L_3\dot{\theta}_3^2 \sin\theta_3 + L_6\dot{\theta}_6^2 \sin\theta_6 + L_{eq}\ddot{\theta}_{eq} \cos\theta_{eq} + L_3\ddot{\theta}_3 \cos\theta_3 + L_6\ddot{\theta}_6 \cos\theta_6 \quad (29)$$

Considering the same methodology, the center of mass acceleration of the robot's other links are written as:

$$\ddot{x}_3 = -L_{eq}\dot{\theta}_{eq}^2 \cos\theta_{eq} - a_3\dot{\theta}_3^2 \cos\theta_3 - L_{eq}\ddot{\theta}_{eq} \sin\theta_{eq} - a_3\ddot{\theta}_3 \sin\theta_3 \quad (30)$$

$$\ddot{y}_3 = +L_{eq}\dot{\theta}_{eq}^2 \sin\theta_{eq} + a_3\dot{\theta}_3^2 \sin\theta_3 + L_{eq}\ddot{\theta}_{eq} \cos\theta_{eq} + a_3\ddot{\theta}_3 \cos\theta_3 \quad (31)$$

$$\ddot{x}_4 = -L_{eq}\dot{\theta}_{eq}^2 \cos\theta_{eq} - L_3\dot{\theta}_3^2 \cos\theta_3 - a_4\dot{\theta}_4^2 \cos\theta_4 - L_{eq}\ddot{\theta}_{eq} \sin\theta_{eq} - L_3\ddot{\theta}_3 \sin\theta_3 - a_4\ddot{\theta}_4 \sin\theta_4 \quad (32)$$

$$\ddot{y}_4 = +L_{eq}\dot{\theta}_{eq}^2 \sin\theta_{eq} + L_3\dot{\theta}_3^2 \sin\theta_3 + a_4\dot{\theta}_4^2 \sin\theta_4 + L_{eq}\ddot{\theta}_{eq} \cos\theta_{eq} + L_3\ddot{\theta}_3 \cos\theta_3 + a_4\ddot{\theta}_4 \cos\theta_4 \quad (33)$$

$$\ddot{x}_5 = -L_{eq}\dot{\theta}_{eq}^2 \cos\theta_{eq} - a_5\dot{\theta}_5^2 \cos\theta_5 - L_{eq}\ddot{\theta}_{eq} \sin\theta_{eq} - a_5\ddot{\theta}_5 \sin\theta_5 \quad (34)$$

$$\ddot{y}_5 = +L_{eq}\dot{\theta}_{eq}^2 \sin\theta_{eq} + a_5\dot{\theta}_5^2 \sin\theta_5 + L_{eq}\ddot{\theta}_{eq} \cos\theta_{eq} + a_5\ddot{\theta}_5 \cos\theta_5 \quad (35)$$

$$\ddot{x}_6 = -L_{eq}\dot{\theta}_{eq}^2 \cos\theta_{eq} - L_3\dot{\theta}_3^2 \cos\theta_3 - L_6\dot{\theta}_6^2 \cos\theta_6 - L_{eq}\ddot{\theta}_{eq} \sin\theta_{eq} - L_3\ddot{\theta}_3 \sin\theta_3 - a_6\ddot{\theta}_6 \sin\theta_6 \quad (36)$$

$$\ddot{y}_6 = +L_{eq}\dot{\theta}_{eq}^2 \sin\theta_{eq} + L_3\dot{\theta}_3^2 \sin\theta_3 + L_6\dot{\theta}_6^2 \sin\theta_6 + L_{eq}\ddot{\theta}_{eq} \cos\theta_{eq} + L_3\ddot{\theta}_3 \cos\theta_3 + a_6\ddot{\theta}_6 \cos\theta_6 \quad (37)$$

### A) Deriving dynamic equations

Considering  $F_{ix}$  and  $F_{iy}$  as the horizontal and vertical internal forces between links  $i$  and  $-1$ , and using Newton's Second Law for foot, thigh, and shank of the front swing leg in the  $x$  direction:

$$F_{SWx}^F = m_{SW}^F \ddot{x}_{SW}^F \quad (38)$$

$$F_{4y} = F_{SWx}^F + m_4 \ddot{x}_4 \quad (39)$$

$$F_{3y} = F_{4x} + m_3 \ddot{x}_3 \quad (40)$$

And in  $y$  directions:

$$F_{SWy}^F = m_{SW}^F \ddot{y}_{SW}^F + m_{SW}^F g \quad (41)$$

$$F_{4y} = F_{SWy}^F + m_4 \ddot{y}_4 + m_4 g \quad (42)$$

$$F_{3y} = F_{4y} + m_3 \ddot{y}_3 + m_3 g \quad (43)$$

Writing Newton's Second Law for the hind foot, hind leg, and trunk in the  $x$  direction:

$$F_{SWx}^H = m_{SW}^H \ddot{x}_{SW}^H \quad (44)$$

$$F_{6x} = F_{SWx}^H + m_6 \ddot{x}_6 \quad (45)$$

$$F_{5x} = F_{6x} + m_5 \ddot{x}_5 \quad (46)$$

And in  $y$  directions:

$$F_{SWy}^H = m_{SW}^H \ddot{y}_{SW}^H + m_{SW}^H g \quad (47)$$

$$F_{6y} = F_{SWy}^H + m_6 \ddot{y}_6 + m_6 g \quad (48)$$

$$F_{5y} = F_{6y} + m_5 \ddot{y}_5 + m_5 g \quad (49)$$

Writing Newton's Second Law in a circular direction for stance links ( $i=1,2$ ) around the contact point, and for swing links ( $i=3,4,5,6$ ) around the centre of mass, respectively:

$$T_6 = I_6 \ddot{\theta}_6 - F_{6x} a_6 \sin\theta_6 + F_{6y} a_6 \cos\theta_6 - F_{SWx} (L_6 - a_6) \sin\theta_6 + F_{SWy} (L_6 - a_6) \cos\theta_6 \quad (50)$$

$$T_5 = I_5 \ddot{\theta}_5 - F_{5x} a_5 \sin\theta_5 + F_{5y} a_5 \cos\theta_5 - F_{6x} (L_5 - a_5) \sin\theta_5 + F_{6y} (L_5 - a_5) \cos\theta_5 + T_6 \quad (51)$$

$$T_4 = I_4 \ddot{\theta}_4 - F_{4x} a_4 \sin\theta_4 + F_{4y} a_4 \cos\theta_4 - F_{SWx} (L_4 - a_4) \sin\theta_4 + F_{SWy} (L_4 - a_4) \cos\theta_4 \quad (52)$$

$$T_3 = I_3 \ddot{\theta}_3 - F_{3x} a_3 \sin\theta_3 + F_{3y} a_3 \cos\theta_3 - F_{4x} (L_3 - a_3) \sin\theta_3 + F_{4y} (L_3 - a_3) \cos\theta_3 + T_4 \quad (53)$$

$$T_1 = I_{eq} \ddot{\theta}_{eq} + m_1 g a_1 \cos\theta_1 + m_2 g (L_1 \cos\theta_1 + a_2 \cos\theta_2) - F_{3x} (L_1 \sin\theta_1 + L_2 \sin\theta_2) + F_{3y} (L_1 \cos\theta_1 + L_2 \cos\theta_2) - F_{5x} (L_1 \sin\theta_1 + L_2 \sin\theta_2) + F_{5y} (L_1 \cos\theta_1 + L_2 \cos\theta_2) \quad (54)$$

### References

- [1].McGeer, T., 1990, "Passive Dynamic Walking," Int. J. Rob. Res., 9(2), pp. 62–82.
- [2].McGeer, T., 1990, "Passive walking with knees," Robotics and Automation, 1990. Proceedings., 1990 IEEE International Conference on, IEEE, pp. 1640–1645.
- [3].Kamath, a. K., and Singh, N. M., 2009, "Impact dynamics based control of compass gait biped," 2009 Am. Control Conf., (1), pp. 4357–4360.
- [4].Farrell, M., "Control of the Compass Biped via Hip Actuation and Weight Perturbation for Small Angles and Level Ground Walking," media.mit.edu.
- [5].Spong, M., 1999, "Passivity based control of the compass gait biped," Proc. IFAC World Congr. Beijing, China, pp. 19–24.
- [6].Spong, M. W., and Bhatia, G., 2003, "Further

- results on control of the compass gait biped,” Proc. 2003 IEEE/RSJ Int. Conf. Intell. Robot. Syst. (IROS 2003) (Cat. No.03CH37453), 2.
- [7]. Asano, F., and Yamakita, M., 2001, “Virtual gravity and coupling control for robotic gait synthesis,” IEEE Trans. Syst. Man, Cybern. - Part A Syst. Humans, 31(6), pp. 2–7.
- [8]. Asano, F., Yamakita, M., Kamamichi, N., and Luo, Z.-W., 2004, “A Novel Gait Generation for Biped Walking Robots Based on Mechanical Energy Constraint,” IEEE Trans. Robot. Autom., 20(3), pp. 565–573.
- [9]. Asano, F., and Yamakita, M., 2005, “Biped gait generation and control based on a unified property of passive dynamic walking,” IEEE Trans. Robot., 21(4), pp. 754–762.
- [10]. Asano, F., and Luo, Z., 2006, “On Energy-Efficient and High-Speed Dynamic Biped Locomotion with Semicircular Feet,” 2006 IEEE/RSJ Int. Conf. Intell. Robot. Syst., pp. 5901–5906.
- [11]. Harata, Y., Asano, F., Luo, Z.-W., Taji, K., and Uno, Y., 2007, “Biped gait generation based on parametric excitation by knee-joint actuation,” 2007 IEEE/RSJ Int. Conf. Intell. Robot. Syst., pp. 2198–2203.
- [12]. Shkolnik, A., and Tedrake, R., 2007, “Inverse Kinematics for a Point-Foot Quadruped Robot with Dynamic Redundancy Resolution,” Proc. 2007 IEEE Int. Conf. Robot. Autom., pp. 4331–4336.
- [13]. Kuo, A. D., 2007, “The six determinants of gait and the inverted pendulum analogy: A dynamic walking perspective,” Hum. Mov. Sci., 26(4), pp. 617–656.
- [14]. Griffin, T. M., Main, R. P., and Farley, C. T., 2004, “Biomechanics of quadrupedal walking: how do four-legged animals achieve inverted pendulum-like movements?,” J. Exp. Biol., 207(Pt 20), pp. 3545–58.
- [15]. Mu, X., and Wu, Q., 2006, “On impact dynamics and contact events for biped robots via impact effects,” IEEE Trans. Syst. Man. Cybern. B. Cybern., 36(6), pp. 1364–1372.
- [16]. Shah, S., Saha, S., and Dutt, J., 2012, “Modular framework for dynamic modeling and analyses of legged robots,” Mech. Mach. Theory, 49, pp. 234–255.
- [17]. Wang, X., Li, M., Wang, P., Guo, W., and Sun, L., 2012, “Bio-Inspired Controller for a Robot Cheetah with a Neural Mechanism Controlling Leg Muscles,” J. Bionic Eng., 9(3), pp. 282–293.